Diffusion and trapping in one-dimensional disordered systems: Transient-grating technique

A. Bourdon, J. Duran, F. Pellé,* and D. de Viry
Laboratoire d'Optique de la Matière Condensée
(Equipe de Recherche No. 133 du Centre National de la Recherche Scientifique),
Université Pierre et Marie Curie, Tour 13, 4 place Jussieu, F-75230 Paris (Cédex) 05, France
(Received 9 April 1984)

The incoherent diffusion problem is studied on one-dimensional chains where both trapping and diffusion follow locally a regular Fick's law. When disorder parameters are included in the calculation, the analysis of the results of picosecond transient-grating experiments displays different behavior depending on the interfringe distance of the transient grating. We propose various theoretical considerations which hold in the general case. We derive an exact calculation of the observable effects in the case of shallow traps and uniform diffusion. Starting from a computer simulation, we consider the general case involving both diffusion and trapping on various segments. We show that the consideration of the small- and large-interfringe-distance limits is quite fruitful and leads to an experimental determination of the basic parameters of disorder, such as the mean diffusion lengths, the trap-to-trap distance, the trapping radius, and the diffusion coefficients. This work reveals the great efficiency of picosecond transient-grating techniques when one deals with one-dimensional disordered systems. Additionally it demonstrates that care should be taken in experiments involving interfringe distances that are of the same order of magnitude as the characteristic lengths of the problem.

I. INTRODUCTION

The recent development of ultrafast picosecond spectroscopy introduced a powerful tool for the study of energy migration or transport in condensed matter. Although transport phenomena such as one- or three-dimensional semiconductors, chemical reactivity, diffusion, and chemical reactions in porous media, etc., concern different fields of study, all these processes are closely related to the more general problem of disorder in condensed phases, where the existence of both diffusion or transport and trapping impurities interact in an intricate process.[1–6]

From a general point of a view, most of the reported experiments have been unable to bring a real quantitative description of the basic mechanisms governing the interplay between transport and trapping. This is mainly due to the fact that in all these works the characteristic length scale of the measurements was much larger than the averaged mean diffusion length, thereby leading to a macroscopic understanding of the processes. In turn, the essential characteristic parameters of the disorder could never have been estimated through analysis of these experiments.

The introduction by Fayer *et al.*[7,8] of picosecond transient experiments opened a new field of growing interest. As far as solid-state or viscous materials are concerned, the ability of picosecond transient-grating experiments to provide both good time, as well as space, resolution may be a definite advantage when dealing with disorder problems.

In particular, the geometrical resolution of a typical transient-grating experiment (up to 0.2 μm) turns out to be, in most instances, of the same order of magnitude or smaller than the mean distance between dislocations and traps in many materials. Keeping this important feature in mind, the basic equations governing the process must be reconsidered. The main purpose of this paper is to provide a theoretical basis for understanding these transient-grating experiments on systems displaying these kinds of inhomogeneities.

Following a conventional macroscopic approach for incoherent energy diffusion in one-dimensional material, a continuous-decay process occurring simultaneously with diffusion is assumed. Under these circumstances, the time dependence of the excited-state distribution $N(x,t)$ is described using the classical Fick's law:

$$\frac{\partial N(x,t)}{\partial t}=D\frac{\partial^2 N(x,t)}{\partial x^2}-\frac{N(x,t)}{\tau}\ , \tag{1.1}$$

where D stands for the diffusion constant and τ stands for the excited-system lifetime. Following this macroscopic scheme, both parameters D and τ are considered to be constant throughout the diffusion range. As shown recently,[9] picosecond transient-grating experiments turn out to be unique in the sense that they can provide separate information about the decay times and the diffusion constants D. Actually, these experiments consist of intersecting two coherent laser beams on the sample at time $t=0$ and at angle θ, producing a sinusoidal distribution of excited states in the sample with a period Λ given by

$$\Lambda=\frac{\lambda}{2\sin(\theta/2)}\ ,$$

where λ is the wavelength of the excitation laser. In turn, this distribution acts as a transient grating which is able

to diffract a delayed probe beam, the intensity of which is monitored so as to obtain a direct measurement of the grating printed at time $t=0$. Now, the contrast of this grating decays following two competitive processes. The first deals with the normal decay of the excited states in the material, and the second relates to the diffusion process whereby the excited maxima tend to transfer energy to the unexcited part of the sinusoidal distribution. Under these circumstances, the decay of the probe-beam intensity has been shown[9] to follow an exponential law with a time constant T_0 given by

$$\frac{1}{T_0}=2\left[\frac{1}{\tau}+\frac{4\pi^2 D}{\Lambda^2}\right]. \tag{1.2}$$

As shown previously, a set of experiments involving various angles θ gives a straightforward estimate of both the decay times τ and the diffusion constants D.

As far as homogeneous material, or systems where the inhomogeneities are much smaller than the characteristic length parameter (Λ) of the measurement, are concerned, these equations are expected to give a realistic description of the involved process. The question of whether the Λ interfringe distance is of the same order of magnitude or smaller than the various pertinent distances in the sample is still to be answered. In turn, as we show in the following, the interpretation of the transient-grating experiments can elucidate unique information about the very nature of the disorder in these materials.

Before dealing with more quantitative estimates of the various processes likely to be encountered in real materials, we first give a definition of and better insight into what, in the following, we call the small- and large-interfringe-distance limits.

A. Small- and large-interfringe-distance limits in transient-grating experiments

As far as transient-grating experiments are concerned, we must distinguish two extreme separate cases which can be solved by starting from simple arguments. The first deals with highly disordered systems where the mean free path for diffusion or any other characteristic length of the problem turns out to be much smaller than the distance Λ between two maxima at time $t=0$ of the printed excited-state grating.

Considering the basic equations of the problem, if D_i stands for the diffusion parameter at abscissa i and if D_i is supposed to run over a homogeneous segment i, the length of which is l_i, the transient-grating signal is expected to decay exponentially with a single time constant T_L given by

$$\frac{1}{T_L}=\frac{8\pi^2}{\Lambda^2}\frac{\sum_i l_i D_i}{\sum_i l_i}, \tag{1.3}$$

as far as any l_i is smaller than the interfringe Λ (see Fig. 1).

In turn, if the characteristic diffusion lengths are much larger than the experimental interfringe distance Λ (small-interfringe-distance limit), we will obtain a transient-grating signal S which decreases following a multiexponential decay given by

$$S\propto\left[\frac{\sum_i l_i\exp(-t4\pi^2 D_i/\Lambda)}{\sum_i l_i}\right]^2. \tag{1.4}$$

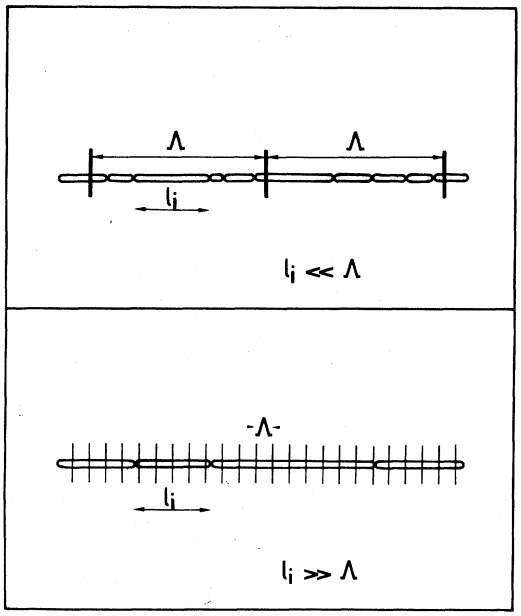

FIG. 1. Diagram showing the interplay between the interfringe distance Λ and the mean diffusion length l_i.

In other words, the large-interfringe-distance limit is, as far as the detailed nature of the disorder is unknown, equivalent to the classical result reported in Eq. (1.2). Seen from the experimental point of view, disorder seems to be averaged due to the lack of spatial resolution.

On the contrary, the small-interfringe-distance limit allows us to gain insight into the very nature of disorder due to the nonexponential behavior of the signal.

It turns out that both Eqs. (1.3) and (1.4) contain an excessively large number of unknown parameters which are very difficult to extract from experimental results. Our purpose now is to reduce the number of the pertinent parameters by considering real experimental situations.

B. Parameters of the problem: Some real situations

Seen from a purely mathematical standpoint, the solution of the most general situation would involve the complete resolution of Eq. (1.1) where both D and τ would depend on the x coordinate. Various attempts have been made in this regard. In particular, the problem where the diffusion constant continuously changes on the x axis has been solved at least in the case of particular dependences.[1,3]

Fortunately, it happens that the real problem can be approached most simply by considering only two kinds of domains involving both diffusion and decay in a classical

scheme. Figure 2 shows a number of important situations where only a pair of different constants must be considered. This is mainly due to the fact that we are considering essentially two different processes, i.e., diffusion (or transport) and trapping. As explained in the caption of Fig. 2, all the cases considered can be computed using only two different pairs of parameters. D_1,D_2 and τ_1,τ_2, including, of course, the diffusion lengths l_1 and l_2. Now, if we refer to Fig. 2 we can describe all cases, (A), (B), (C), and (D), as follows:

(A) $D_1=D_2=D$ (nonzero), $\tau_1=\infty$, and finite τ_2 ,

(B) $D_1\neq 0$, $D_2=0$, $\tau_1=\infty$, and finite τ_2 ,

(C) $D_1\neq 0$, $D_2=0$, and $\tau_1=\tau_2=\infty$,

(D) $D_1\neq 0$, $D_2\neq 0$, and $\tau_1=\tau_2=\infty$.

Actually, case (A) can be completely solved analytically, whereas cases (B), (C), and (D) involve very cumbersome calculations. In order to give a complete description of the expected effects involving the general case when D_1,D_2 and τ_1,τ_2 are all nonzero or infinite, we have dealt with the most general case by setting up a computer simulation as described in Sec. IV. However, various pertinent and general conclusions can be extracted from the consideration of the general mathematical problem. In addition, a complete calculation dealing with case (A) will lead to a better understanding of the processes.

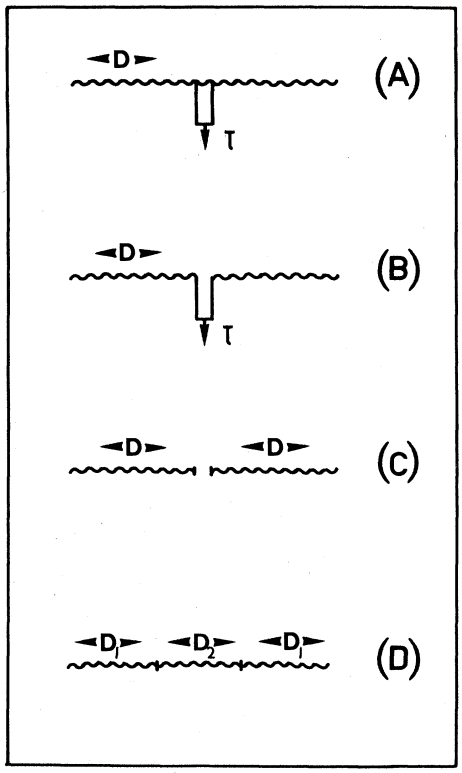

FIG. 2. Schematic illustration of the various relevant processes displaying both diffusion (transport) and (or no) trapping. Case (A) corresponds to a diffusion process in a material where the D parameter is constant and extends over all traps (shallow traps). Case (B) deals with a material containing deep traps: The diffusion occurs with a constant diffusion parameter, and the trapping process is irreversible. Case (C) refers to a material containing dislocations: The system is made up of isolated systems where the diffusion occurs freely. Case (D) shows the example of a purely heterogeneous linear chain displaying two different diffusion constants D_1 and D_2.

II. GENERAL TRENDS: ANALYTICAL SOLUTIONS

The excited-state density $N(x,t)$, which is created by an external excitation $E(x,t)$, is governed by the following differential equation:

$$-\frac{\partial}{\partial x}\left[D(x)\frac{\partial N}{\partial x}\right]+\frac{1}{\tau(x)}N+\frac{\partial N}{\partial t}=E\ , \tag{2.1}$$

where the diffusion coefficient $D(x)$ and lifetime $\tau(x)$ depend on the x position in the linear system. Since Eq. (2.1) depends linearly on N, its solutions can be written as

$$N(x,t)=\int\int E(x',t-t')G(x,x';t')dx'\,dt'\ . \tag{2.2}$$

Our purpose here is to determine the properties of the Green response function from those of $D(x),\tau(x)$; conversely, we will analyze the characteristic parameters of the system which can be derived from picosecond transient-grating experiments.

A. Time evolution of the excited-state density

Considering Eq. (2.1), we tentatively define a diffusion-trapping (DT) operator H,

$$H=-\frac{\partial}{\partial x}\left[D(x)\frac{\partial}{\partial x}\right]+\frac{1}{\tau(x)}\ , \tag{2.3}$$

which allows us to rewrite Eq. (2.1) as

$$(H-i\omega)N'(x,\omega)=E'(x,\omega)\ , \tag{2.4}$$

where $N'(x,\omega)$ and $E'(x,\omega)$ are time Fourier transforms of $N(x,t)$ and $E(x,t)$, respectively.

Provided that the system is periodic with a sufficiently large period L, and that the Born cyclic conditions are taken into account, the DT operator H is Hermitian; let ψ_n and h_n be its normalized eigenfunctions and values, respectively. As $D(x)$ and $\tau(x)$ are strictly positive, it follows that all the h_n are also strictly positive.

We define P_n as the projection operator on ψ_n. Equation (2.4) becomes

$$N'(x,\omega)=\sum_n \frac{1}{h_n-i\omega}P_nE'(x,\omega)\ . \tag{2.5}$$

In turn, $N(x,t)$ may be calculated from

$$N(x,t)=\int_{-\infty}^{+\infty}dt'\sum_n\left[P_n\int_{-\infty}^{+\infty}e^{-i\omega(t-t')}E'(x,\omega)d\omega\right]\times\left[\frac{1}{2\pi}\int_{-\infty}^{+\infty}\frac{e^{-i\omega' t}}{h_n-i\omega'}d\omega'\right]\ .$$

Since the set of the h_n eigenvalues is always positive, we can write

$$\frac{1}{2\pi}\int_{-\infty}^{+\infty}\frac{e^{-i\omega t}}{h_n-i\omega}d\omega=\Theta(t)e^{-h_n t},$$

where $\Theta(t)$ is the usual Heaviside unit step function. Then Eq. (2.2) may be symbolically written as

$$N(x,t)=\int_{-\infty}^{+\infty}dt'\,G(t')E(x,t-t'), \tag{2.6}$$

where $G(t)$ is now an operator defined by

$$G(t)=\Theta(t)e^{-Ht}, \tag{2.7}$$

or, more classically,

$$G(x,x';t)=\Theta(t)\left[\sum_n \psi_n(x)e^{-h_n t}\psi_n^*(x')\right]. \tag{2.8}$$

This equation confirms the idea that the decay of the response function is made up of an infinite number of exponential functions excluding any oscillatory behavior.

B. Transient-grating experiment: Intensity of the diffracted light

In a transient-grating experiment, the $E(x,t)$ distribution can be factorized as

$$E(x,t)=\frac{e(t)}{2}\left[1+\cos\left[\frac{2\pi x}{\Lambda}+\varphi\right]\right]. \tag{2.9a}$$

As we shall see later, $N(x,t)$ can be approximated as

$$N(x,t)=N_0(t)+N_1(t)\cos\left[\frac{2\pi x}{\Lambda}+\varphi'\right].$$

$N_0(t)$ and $N_1(t)$ result from a convolution of $e(t)$ with two different Green functions. In a general way, the E and N distributions can be expanded as

$$E(x,t)=e(t)\left[\sum_q a_q e^{iqx}\right], \tag{2.9b}$$

$$N(x,t)=\sum_q N_q(t)e^{iqx}. \tag{2.10}$$

The $N_q(t)$ components are deduced from $e(t)$ by convolution with a response function $R_q(t)$:

$$N_q(t)=\int_0^{\infty}R_q(t')e(t-t')dt'. \tag{2.11}$$

Equations (2.8)–(2.11) allow us to obtain $R_q(t)$ by making the identification

$$R_q(t)=\sum_{q'}G_{q,q'}(t)a_{q'}, \tag{2.12}$$

where

$$G_{q,q'}(t)=\sum_n \Phi_{q,n}e^{-h_n t}\Phi_{q',n}^* \tag{2.13}$$

and

$$\Phi_{q,n}=\frac{1}{\sqrt{L}}\int_0^L e^{-iqx}\psi_n(x)dx. \tag{2.14}$$

Considering Eq. (2.13), we can isolate three interesting properties of the Green function $G_{q,q'}(t)$.

(i) In particular, near the time origin we find

$$G_{q,q'}(0^+)=\delta_{q,q'}\ \text{ and }\ G_{q,q'}(t>0)\neq\delta_{q,q'}, \tag{2.15}$$

and, consequently, $R_q(0^+)=a_q$. Therefore the excited-state density that can be observed immediately after a very short excitation pulse will exactly mimic the spatial distribution of the excitation.

Considering Eq. (2.15), it is important to remark that the experimental conditions for observing the diffracted light may elucidate much interesting information. In other words, if we analyze the diffracted light under normal Bragg conditions, the signal will show up immediately after the excitation pulse. In turn, the analysis of the diffracted light at other angles will exhibit a time lag which is likely to give information about the disorder characteristics of the system.

(ii) Now, if we consider the first-order derivative $G_{q,q'}(t)$, and introduce

$$V(x)=\frac{1}{\tau(x)}, \tag{2.16}$$

we find

$$\left[\frac{dG_{q,q'}(t)}{dt}\right]_{t=0^+}=-[qq'\tilde{D}(q-q')+\tilde{V}(q-q')], \tag{2.17}$$

where $\tilde{D}(q)$ and $\tilde{V}(q)$ stand for the space Fourier transforms of $D(x)$ and $V(x)$. Particularly, at $q=q'$ we find

$$\left[\frac{dG_{q,q}(t)}{dt}\right]_{t=0^+}=-\left[q^2\langle D(x)\rangle+\left\langle\frac{1}{\tau(x)}\right\rangle\right], \tag{2.18}$$

which obviously leads to the well-known results[9] when D and τ are independent of x.

(iii) At long-time values, the $G_{q,q}(t)$ function ends up in a single exponential decay, the exponent of which is given by the smallest eigenvalue h_n, for which $\Phi_{n,q}$ is non zero.

The diffracted-light intensity $I_q(t)$ is proportional to the squared modulus of $N_q(t)$ [cf. Eq. (2.11)]:

$$I_q(t)=\propto |N_q(t)|^2. \tag{2.19}$$

For a very short pulsed excitation, $N_q(t)$ is proportional to $R_q(t)$, and $I_q(t)$ is simply a sum of cross products of $G_{q,q'}(t)$ [cf. Eq. (2.12)]:

$$I_q(t)=\beta\sum_{q',q''}a_{q'}a_{q''}^*G_{q,q'}(t)G_{q,q''}(t). \tag{2.20}$$

In a transient-grating experiment, there are only three nonzero a_q components [cf. Eq. (2.9a)]:

$$a_0=\tfrac{1}{2},\quad a_{q_0}=e^{i\varphi}/4,\quad a_{-q_0}=a_{q_0}^*,$$

where $q_0=2\pi/\Lambda$.

The φ phase is a measure of the relative position of the holographic grating and the linear chain. The average value over a large number of experiments involving random φ phases will lead to

$$\langle I_{q_0}(t)\rangle=\frac{\beta}{16}\left[|G_{q_0,q_0}(t)|^2+4|G_{q_0,0}(t)|^2+|G_{q_0,-q_0}(t)|^2\right]. \quad (2.21)$$

This averaged function over many experiments should be equivalent to considering a single experiment on a random chain with the same values for $\langle D(x)\rangle$ and for $\langle 1/\tau(x)\rangle$.

These parameters can be separately evaluated by performing experiments at different Λ values of the transient grating. Immediately after a very short excitation pulse, $I_{q_0}(t)$ is only governed by $G_{q_0,q_0}(t)$ because the other two terms $G_{q_0,0}(t)$ and $G_{q_0,-q_0}(t)$ turn out to be proportional to time, so that

$$\ln\left[\frac{I_{q_0}(t)}{I_{q_0}(0)}\right]=-2\left[\langle D\rangle\frac{4\pi^2}{\Lambda^2}+\left\langle\frac{1}{\tau}\right\rangle\right]t . \quad (2.22)$$

III. PERIODIC ONE-DIMENSIONAL MODELS

The response function of the system is determined by the set of the eigenvalues and eigenfunctions of the diffusion-trapping operator [Eq. (2.3)]. These quantities cannot be evaluated analytically in a random system. However, the response function of a stationary (versus x) random system is very close to the average of response functions of periodical systems which are built up with the same elements and the characteristics of which are equal to the averaged properties of this random system. It is the reason why we present here a short study of the response of some periodical systems. Let l be the period of the system. As in solid-state physics, the eigenvalues of the DT operator form a band structure. They are labeled with two indices in the reduced-zone scheme: n, a band number; and k, a one-dimensional "vector" in the Brillouin zone:

$$H\psi_{n,k}=h_{n,k}\psi_{n,k} . \quad (3.1)$$

Partial Green functions of $G_{q,q'}(t)$ may be then written as [cf. Eq. (2.13)]

$$G_{q,q'}(t)=\sum_{n,k}\Phi_{q;n,k}e^{-h_{n,k}}\Phi^*_{q';n,k} . \quad (3.2)$$

Owing to the selection rules, matrix elements $\Phi_{q;n,k}$ are nonzero only if

$$k=q+m\frac{2\pi}{l}\quad (m \text{ integer}) . \quad (3.3)$$

All the models which are described in Sec. I exhibit two kinds of regions where D and τ are constant. Let l_1 and l_2 be their averaged lengths in the random chain. The unit cell of the simplest periodic chain that best simulates the random one is made of two zones. Their lengths are l_1 and l_2. In each region i (1 or 2), the eigenfunctions are solutions of

$$D_i\frac{\partial^2\psi_{n,k}}{\partial x^2}-(V_i-h_{n,k})\psi_{n,k}=0 . \quad (3.4)$$

They can be written as

$$\psi_{n,k}=A_ie^{K_ix}+B_ie^{-K_ix} . \quad (3.5)$$

Equation (3.4) resembles a constant-potential Schrödinger equation. This analogy is not perfect because the equivalent of the particle mass $(1/2D_i)$ may differ in both regions. Furthermore, the continuity conditions between two regions differ slightly from those of quantum mechanics because excited-state current depends on diffusion coefficient: $\psi_{n,k}(x)$ and $D(x)(\partial\psi_{n,k}/\partial x)$ are continuous at the boundary. Nevertheless, this model resembles that of Kronig and Penney, and its solution is very similar. Let V_1 be lesser than or equal to V_2, and we introduce

$$K_i^2=-k_i^2=\frac{V_i-h_{n,k}}{D_i} . \quad (3.6)$$

As in quantum mechanics there are three possibilities for $h_{n,k}$ to solve Eq. (3.4). The first, when $h_{n,k}$ is lower than V_1, has no normalizable solution. In the two other cases, we find, for $V_1\le h_{n,k}\le V_2$,

$$\cos(k_1l_1)\cosh(K_2l_2)-\frac{D_1k_1^2-D_2^2K_2^2}{2D_1k_1D_2K_2}\times\sin(k_1l_1)\sinh(K_2l_2)=\cos(kl) , \quad (3.7)$$

and for $V_1\le V_2\le h_{n,k}$,

$$\cos(k_1l_1)\cos(k_2l_2)-\frac{D_1k_1^2+D_2^2k_2^2}{2D_1k_1D_2k_2}\times\sin(k_1l_1)\sin(k_2l_2)=\cos(kl) . \quad (3.8)$$

Thus, Kronig-Penney-like models can be completely solved. The entire set of exponents is determined by Eqs. (3.6)—(3.8). The Bloch theorem and continuity conditions determine the A_i and B_i coefficients of $\psi_{n,k}$ [Eq. (2.5)] and, consequently, $G_{q,q'}(t)$.

We have studied more precisely the particular case when region 2 is very narrow but has a very short lifetime so that l_2/τ_2 cannot be neglected. This is an excited-state recombination-center model. Equation (3.7) then becomes

$$\cos(k_1l)+P\frac{\sin(k_1l)}{k_1l}=\cos(kl) , \quad (3.9)$$

where

$$P=\frac{ll_2}{2\tau_2D_1} . \quad (3.10)$$

P is a dimensionless parameter which does not depend on D_2; this is natural because region 2 is too narrow to let excited states be diffused. The $h_{n,k}$ exponents can be written as [Eq. (3.6)]

$$h_{n,k}=\frac{1}{\tau_1}+k_1^2D ,$$

or

$$h_{n,k}=\frac{1}{\tau_1}+\frac{z}{t_0}\ , \tag{3.11}$$

where

$$z=\left[\frac{k_1 l}{2\pi}\right]^2 \tag{3.12}$$

and

$$t_0=\frac{l^2}{4\pi^2 D}\ . \tag{3.13}$$

This notation allows a simple presentation of the results: $1/\tau_1$ is simply a general shift for the exponents, and t_0 is chosen in order to be independent of Λ. All results can be given by dimensionless curves:

$$y=\left[\ln\left[\frac{I_{q_0}(t)}{I_{q_0}(0)}\right]+2\frac{t}{\tau_1}\right]=f(t/t_0)\ . \tag{3.14}$$

The set of z roots is determined by only two parameters, P and a, where

$$a=\Lambda/l\ , \tag{3.15}$$

The $\Phi_{q_0;n,k}$ coefficients could be determined by the rather complicated method of Eqs. (2.14) and (3.5). We have found, by following another type of calculation, that

$$|\Phi_{q_0;n,k}|^2=\left[(1-a^2z)^2\sum_{m=-\infty}^{+\infty}\frac{1}{[(1+ma)^2-a^2z]^2}\right]^{-1}\ . \tag{3.16}$$

Decay curves for

$$y=\ln\left[\frac{I_{q_0}(t)}{I_{q_0}(0)}\right]+\frac{2t}{\tau_1}$$

have been established by using all these formulas. We present in Fig. 3 a set of curves calculated for different values of a, but at the same value of P [$0.2(2\pi^2)$]. Three comments can be made.

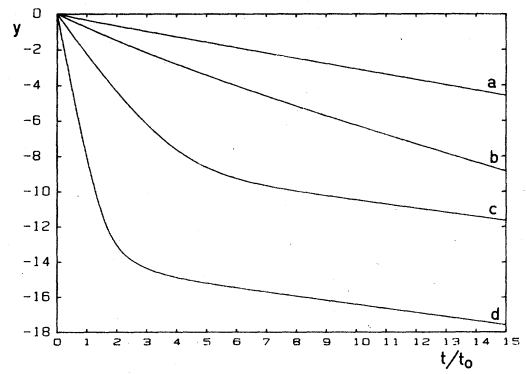

FIG. 3. Theoretical decay curves in a periodic (A)-type chain. Parameter values as follows. $P=0.2(2\pi^2)$. *a*, $\Lambda/l=5$; *b*, $\Lambda/l=2$; *c*, $\Lambda/l=1$; *d*, $\Lambda/l=0.5$. $y=\ln[I_d(t)/I_d(0^+)]+2t/\tau_1$ versus t/t_0.

(a) At the origin, using Eq. (2.22), we find

$$y=-2\left[\frac{t}{t_0}\right]\left[\frac{1}{a^2}+\frac{P}{2\pi^2}\right] \tag{3.17}$$

by noticing [cf. Eq. (3.10)]

$$\left\langle\frac{1}{\tau}\right\rangle=\frac{1}{l}\left[\frac{l_1}{\tau_1}+\frac{l_2}{\tau_2}\right]=\frac{1}{\tau_1}+2P\frac{D_1}{l^2}\ .$$

Equation (3.17) is well verified by Fig. 3.

(b) The same formula [Eq. (3.17)] also gives the decay function of excited states without de-excitation centers only by setting $P=0$:

$$y_D=-\frac{2}{a^2}\left[\frac{t}{t_0}\right]\ . \tag{3.18}$$

This equation is true for all t/t_0. For all values of a we find that $y<y_D$ at the beginning of the decay. After some time and for a smaller than or equal to 2, we find the paradoxical result that the decay turns out to be slowed down by the de-excitation centers.

(c) This paradox is related to the directions of the asymptotes. Their slopes are proportional to the lowest eigenvalue $h_{1,k}$ in the Kronig-Penney band structure. At first, k is determined from a [cf. Eq. (3.3)] according to

$$-\frac{1}{2}<\frac{kl}{2\pi}=\frac{1}{a}+m\le\frac{1}{2}\quad (m\ \text{integer})\ . \tag{3.19}$$

For the different values of a in Fig. 3, we find

$$(a,\ kl/2\pi)=(0.2,0),\ (0.5,0),\ (1,0),\ (2,0.5),\ (5,0.2)\ .$$

Asymptotes for $a=0.5$ and 1 are parallel because they correspond to the same $h_{1,k=0}$ value. Similarly, since the lowest band is very flat around $k=0$, $h_{1,k}$ is not very far from $h_{1,0}$ for $a=5$; this also gives an asymptote parallel to the first ones. On the contrary, for $a=2$, kl is equal to π. In that case, $k_1 l$ is also equal to π and $z=\frac{1}{4}$ whatever P. This corresponds to a higher value of $h_{1,k}$ and, consequently, to a steeper asymptote, as can be verified in Fig. 3.

Unfortunately, the preceding analytical calculation turns out to be very cumbersome when dealing with the situations referred to as cases (B), (C), and (D) in Fig. 2. In order to provide a more complete set of data corresponding to frequently observed situations, we have derived a computer-simulation procedure which we now describe.

IV. COMPUTER SIMULATION

A. Simulation procedure

Keeping in mind the arguments developed in Sec. I, we are now concerned with a diffusion problem on a linear chain containing two types of segments, labeled 1 or 2.

Under these circumstances, the relevant parameters are the following.

(1) The central value of the cluster lengths (l_1,l_2), the distribution of which is supposed to be Gaussian with variance measured by Δl_1 and Δl_2.

(2) The relative concentrations of the two types of segments which are randomly introduced in the elaboration of the chain:

$$C_{1,2}=\frac{N_{1,2}}{N_1+N_2}\ , \tag{4.1}$$

N_1 (N_2) being the number of segments labeled 1 (2). Another relevant definition for concentration refers to the number of particles pertaining to the segments, defined by

$$C'_{1,2}=\frac{N_{1,2}l_{1,2}}{N_1l_1+N_2l_2}\ . \tag{4.2}$$

(3) The diffusion constants D_1 and D_2 relative to the diffusion (or transport) process along segments 1 and 2.

(4) The lifetimes τ_1 and τ_2 corresponding to the decay of the excitation on the two segments.

In order to simulate the transient-grating experiment, a periodic grating of excited states is impressed on the chain at time $t=0$ with a sinusoidal distribution following

$$N(x,\ t=0)=\tfrac{1}{2}[1+\cos(2\pi x/\Lambda)]\ . \tag{4.3}$$

As time passes, the excited-state grating will evolve according to a pair of differential equations similar to Eq. (1.1), but with different parameters on different segments. Taking into account the necessary boundary conditions between two adjacent different segments, it can be shown that the computer solution may be obtained by using an iteration procedure following

$$N(x_i,t_j)=N(x_i,t_{j-1})\left[1-\frac{dt}{\tau_i}\right]$$

$$+D_i dt[N(x_{i-1},t_{j-1})+N(x_{i+1},t_{j-1})$$

$$-2N(x_i,t_{j-1})]\ , \tag{4.4}$$

where i refers to the label of the segment, and j corresponds to the number of the iteration cycle.

In order to obtain significant results, our calculations were performed on sufficiently long chains containing several thousands of particles. Spurious end effects were avoided using the classical cyclic Born conditions.

It is worth noting here that the computer simulation introduces an artificial quantization of the diffusion process. As the invoked process is necessarily incoherent, it becomes clear that this quantization does not correspond to any realistic feature.

The intensity I_d of the diffracted light is then calculated after each iteration cycle by squaring the first-order real Fourier-transform coefficient of the distribution $N(x,t)$. This procedure has been applied in various relevant situations depicted in Fig. 2.

It was reported earlier that the classical Fick's diffusion law regarding homogeneous media gives rise to pure exponential decays. In order to reveal the deviation of the exponential law, which we expect in disordered materials, the time dependence of the diffracted-light intensity has been plotted on a semilogarithmic scale.

In the following we shall describe the results obtained for typical disordered models.

B. Results of computer simulation

We have checked the validity of the iteration procedure in the above-described computer simulation by solving the classical Fick's diffusion equation where the system continuously diffuses and decays along the chain. The results of these calculations are reported in Fig. 4. As expected, we find a pure exponential behavior, the time constant τ_c of which is given by Eq. (1.2). This accurate fit provides a firm support for more complex situations.

In our computer simulation we restricted the problem to two types of segments so that Eqs. (1.3) and (1.4) reduced to, in the large-interfringe-distance limit,

$$S\propto e^{-t/T}\ , \tag{4.5a}$$

where

$$\frac{1}{T}=2\left[C'_1\left[\frac{1}{T_1}\right]+(1-C'_1)\left[\frac{1}{T_2}\right]\right]$$

and (4.5b)

$$\frac{1}{T_{1,2}}=\frac{1}{\tau_1}+\frac{4\pi^2D_{1,2}}{\Lambda^2}\ ,$$

and, in the small-interfringe-distance limit,

$$S\propto\left[C'_1\exp-\frac{t}{T_1}+(1-C'_1)\exp-\frac{t}{T_2}\right]^2\ . \tag{4.5c}$$

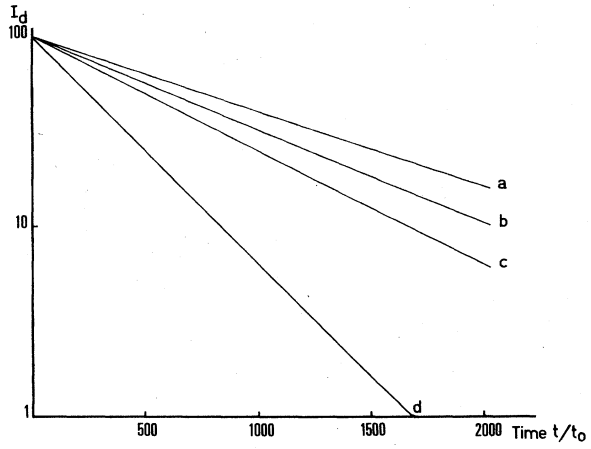

FIG. 4. Results of the simulation for diffusion and trapping processes in an homogeneous medium: diffracted-light intensity versus time for different values of the interfringe spacing (the simulations have been performed with the following set of parameters). $D\,dt=0.2$, and the following Λ values (in a.u.): *a*, 84; *b*, 60; *c*, 48; *d*, 28.

The consideration of these equations in the extreme cases of short and long times can elucidate interesting information. In particular, it can be easily shown that the slope at the origin of the decay curves will provide an averaged quantity involving both diffusion and decay processes weighted by the relative concentration of the two types of domains, as has been demonstrated in Sec. II.

This result also applies in the small-interfringe-distance limit as well as in the large-interfringe-distance limit, and we obtain

$$\left[\frac{\partial S}{\partial t}\right]_0 = 2\left[\frac{C_1'}{T_1} + (1-C_1')\frac{1}{T_2}\right], \tag{4.6}$$

where $\Lambda/d \gg 1$ or $\Lambda/d \ll 1$.

The asymptotic behavior of the decay curves is also quite meaningful, at least in the small-interfringe-distance—limit case: in dealing with Eq. (4.5), we assume that a long time after the excitation pulse the system will display the behavior of a unique exponential because the other processes will have ceased. Thus, at long times after the excitation, we find

$$\ln S = 2\ln C_1' - t/T_1 , \tag{4.7}$$

which, extrapolated to time 0, gives a very convenient method to measure the trap concentration C_1'. As will be clear in the presentation of our results, we have been able to check this result in all the relevant examples we have calculated (e.g., Fig. 2).

Another remarkable feature of this asymptotic behavior is related to the experimental observation of the so-called large- and small-interfringe-distance limits. As can be seen on the calculated curves, the preceding formula is quite sensitive to the Λ/d ratio. In other words, and from the experimental point of view, observation of the dependence of the extrapolated value (at time 0) on the interfringe-distance value while decreasing Λ turns out to be very convenient. The observation of the stabilization of the extrapolated curve will coincide with the occurrence of the small-interfringe-distance limit.

Apart from these considerations, which hold for the entire set of the different experimental situations depicted in Fig. 2, we shall now consider cases (B), (C), and (D), for which we performed the complete simulation, separately, whereas case (A) was treated analytically in Sec. III.

1. *Case (B): Homogeneous diffusion outside deep traps*

This situation corresponds to the very commonly observed systems where the incoherent diffusion process is perturbed by the existence of deep traps (e.g., III-V—compound semiconductors). It should be noted here that our computer simulation takes into account deep traps corresponding to domains where diffusion does not occur ($D_2=0$) and where the excitations (or the particles) disappear with a time constant τ_2. On the other segments the migration is governed by a classical diffusion law with a D_1 parameter and an infinite lifetime τ_1.

The results of the computer simulation are depicted in Fig. 5. In the large-interfringe-distance limit ($\Lambda/d \gg 1$), two time domains must be considered. At first, at short times the excitation (or particles) slowly diffuse in the homogeneous segments. They are then trapped in deep traps and disappear following a fast decay process with a τ_2 time constant. At the end of the process the initially impressed excitations on the deep traps have disappeared; they are only fed by the normal diffusion process from the homogeneous segments, giving rise to a slower decay process, as can be realized from Fig. 5.

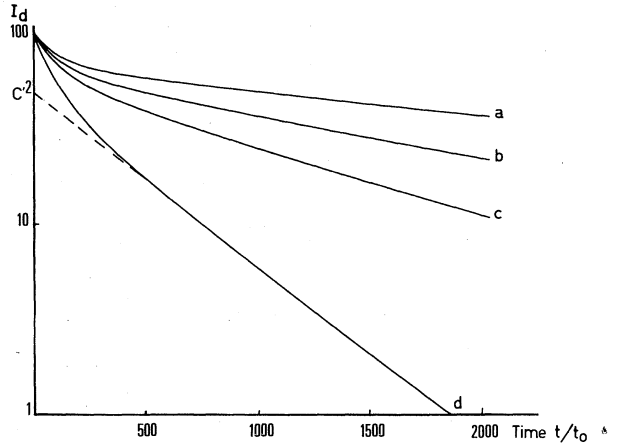

FIG. 5. Homogeneous diffusion outside fast decaying traps: variation of the diffracted intensity with time for different values of the interfringe spacing. The set of injected parameters was concentration of traps $C_2'=0.18$, diffusion constants $D_1\,dt=0.2$ and $D_2\,dt=0$, decay time $dt/\tau_2=10^{-2}$, and domain lengths and variances $L_1=50$, $\Delta L_1=5$ and $L_2=10$, $\Delta L_2=2$. Λ/d values are as follows: *a*, 1.40; *b*, 1; *c*, 0.80; *d*, 0.47.

In the small-interfringe-distance limit ($\Lambda/d \ll 1$), the two processes are completely separated, and, according to Eq. (3.8), the extrapolation of the slow diffusion process at time $t=0$ allows us to determine the concentration of the trapping centers in the linear chain.

2. *Case (C): Homogeneous diffusion outside traps*

This case relates to homogeneous segments separated by randomly distributed defects, and also to materials containing ill-crystallized or dislocation zones where neither diffusion nor normal decay occurs. The results of the computer simulation for this situation are shown in Fig. 6. In the large-interfringe-distance limit, the decay curves nearly display an exponential behavior with a time constant corresponding to an averaged value of the involved diffusion and trapping processes according to Eq. (3.6).

In the small-interfringe-distance limit, the two steps of the migration process are clearly separated. First, the grating of the excited states impressed on the chain at time $t=0$ is smoothed by diffusion on the homogeneous segments so that the slope of the first part of the decay curve is in good agreement with the classical theoretical value given in Eq. (1.2). Actually, the traps act as walls which stop the energy diffusion process so that the excitation will move back and forth between the barriers. This diffusion will stop when the distribution of the excited states becomes uniform. Thus, in the second step the ob-

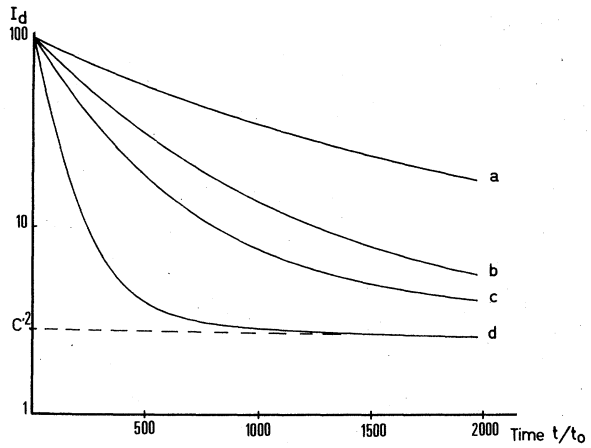

FIG. 6. Homogeneous diffusion outside traps. Transient-grating—diffracted intensity versus time corresponding to various interfringe distances. $C_2'=0.5$, $D_1\,dt=0.15$, $D_2\,dt=0$, $\tau_1=\infty$, $\tau_0=\infty$, and $L_1=50$, $\Delta L_1=5$ and $L_0=10$, $\Delta L_0=2$. Λ/d values are as follows: *a*, 1.40; *b*, 1; *c*, 0.80; *d*, 0.47.

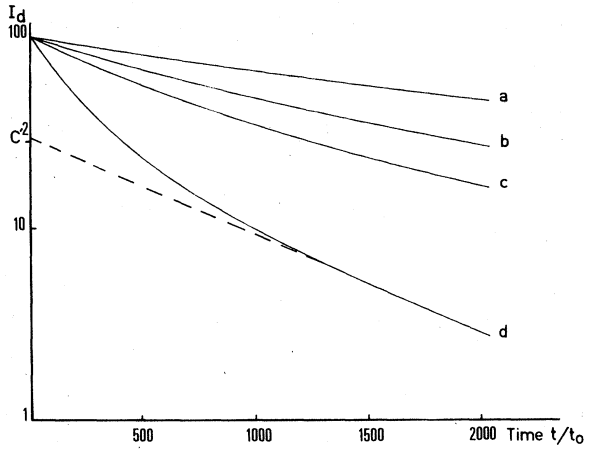

FIG. 7. Inhomogeneous diffusion without trapping effect. Transient-grating—diffracted intensity versus time for different values of interfringe spacing. $C_2'=0.48$, $D_1\,dt=0.07$, $D_2\,dt=0.01$, $\tau_1=\infty$, $\tau_2=\infty$, and $L_1=50$, $\Delta L_1=5$ and $L_0=50$, $\Delta L_0=5$. Λ/d values are as follows: *a*, 0.84; *b*, 0.60; *c*, 0.48; *d*, 0.28.

served signal will only vanish corresponding to the decay process in the traps (if any). Consequently, the mean value of the length of the domains (mean diffusion length) can be extracted in the small-interfringe-distance limit from the interfringe spacing Λ. Another important parameter which is of practical interest in real situations can be obtained from the decay curve; the extrapolation at $t=0$ of the decay curve at long times after the excitation will still provide the determination of the trap concentration.

3. *Case (D): Inhomogeneous diffusion*

This model refers to case (D) in Fig. 2 and corresponds to two kinds of domains randomly distributed along a one-dimensional chain. Both are considered as purely diffusive with diffusion constants D_1 and D_2. In this case no trapping effect is involved. The simulation of the transient-grating experiment has been achieved and the results are given in Fig. 7. The time behavior of the diffracted intensity by the grating in the large-interfringe-distance limit is exponential: The diffusion processes acting on the two domains are averaged, and the decay curve does not reflect the inhomogeneous character of the system. On the other hand, as the Λ/d ratio decreases and the interfringe spacing becomes of the same order as the averaged lengths of the segments, the time dependence of the diffracted intensity deviates from an exponential decay. Under these conditions, the contribution of the diffusion processes occurring in each type of segment are clearly separated according to Eq. (1.3). The averaged lengths of the domains are consequently available from the analysis of these results, and as before, the concentration of the particles belonging to one type of segment is obtained after the extrapolation of the second linear part of the decay curve.

V. CONCLUSION

The physics of condensed materials is currently more and more concerned with the concept of disorder. The geometrical disorder connected with the presence of impurities or traps significantly perturbs the energy- or particle-transport properties. This feature opened a new field of investigation dealing with potentially interesting new devices such as amorphous materials (silicium or glasses) and III-V—compound semiconductors.

The recently developed picosecond technology, and particularly the transient-grating method, is well suited to the analysis of the properties of disordered one-dimensional samples. In particular, the intrinsic spatial resolution associated with this technique allows one to introduce a characteristic length for this kind of measurement. Roughly stated, the system will appear disordered whenever the characteristic diffusion length of the material is larger than the interfringe distance of the transient grating. On the other hand, under the opposite circumstances the system will resemble a homogeneous material.

Actually, this basic idea underlies the entire theoretical work developed in this paper. In order to relate our results to interesting real materials we focused our calculations on incoherent energy diffusion on linear chains which involve shallow traps, deep traps, stopping defects, and inhomogeneous diffusion.

The problem has been treated following two different approaches. First, an analytical solution was proposed. A pseudo-Hamiltonian and its related Green functions were then derived for a periodic system where the diffusion coefficient D and decay time depend on the x coordinate in the linear chain.

A more general computer-simulation procedure was proposed. Some particular cases corresponding to more frequently observed situations were treated.

The results of the complete simulation as well as the

analytical calculation clearly show the pertinence of the Λ/d parameter. We have proved that a careful examination of the decay curves of the diffracted light allows one to obtain an estimate of the trap concentration, the mean trap distance, and, more generally, the characteristic diffusion lengths.

The field of application of this technique has been widely opened toward the analysis of the basic properties of numerous practically interesting materials. It may concern the basic mechanism of the photographic process, the chemical reactivity on surfaces (catalysis problems), and impurity problems in III-V—compound semiconductors.[10]

This work was mainly directed toward one-dimensional systems. It may also be applied to two- or three-dimensional diffusion, provided that a number of minor modifications are made. This important extension is being currently worked out in our laboratory and the results will be published in a planned, forthcoming paper. We hope that the present work will initiate further effort in this vastly interesting field which would deal further with the relationship between transient-grating experiments and disorder in condensed matter.

---

*Present address: Laboratoire de Physico—Chimie de l'Ecole Centrale de Paris (Equipe de Recherche No. 928 du Centre National de la Recherche Scientifique), E.C.A.M., F-92290, Chatenay-Malabry, France.

[1]B. Derrida and Y. Pomeau, Phys. Rev. Lett. **48**, 627 (1982).

[2]J. W. Haus, K. W. Kerr, and J. W. Lyklema, Phys. Rev. B **25**, 2905 (1982).

[3]M. Ya. Azbel, Solid State Commun. **43**, 515 (1982).

[4]S. B. Haley, Phys. Rev. B **25**, 5824 (1982).

[5]S. W. Haan and R. Zwanzig, J. Chem. Phys. **68**, 1879 (1978).

[6]I. Webman and J. Klafter, Phys. Rev. B **26**, 5950 (1982).

[7]M. D. Fayer, in *Picosecond Phenomena III,* Vol. 23 of *Springer Series in Chemical Physics,* edited by K. B. Eisenthal, R. M. Hochstrasser, W. Kaiser, and A. Laubereau (Springer, Berlin, 1982).

[8]D. R. Lutz, K. A. Nelson, C. R. Gochanour, and M. D. Fayer, Chem. Phys. **58**, 225 (1981).

[9]J. R. Salcedo, A. E. Siegman, D. D. Dlott, and M. D. Fayer, Phys. Rev. Lett. **41**, 131 (1978).

[10]C. A. Hoffman, K. Jarasiunas, H. J. Gerritsen, and A. V. Nurmikko, Appl. Phys. Lett. **33**, 536 (1978).